Bestimmung von Kulturpflanzeneigenschaften mittels hyperspektraler Fernerkundung von einem Mikro-UAV

Detection of crop properties by means of hyperspectral remote sensing from a micro UAV

Dragos Constantin[1], Martin Rehak[1], Yosef Akhtman[1], Frank Liebisch[2+]

[1] *Institute of Environmental Engineering, École Polytechnique Fédérale de Lausanne (EPFL), Lausanne, Switzerland*
[2] *Institute of Agricultural Sciences, Federal Institute of Technology Zürich (ETHZ), Universitätsstrasse 2, 8092 Zürich Switzerland*
Email: frank.liebisch@usys.ethz.ch
[+] *Presenter*

The presented poster is based partly on a talk given by Dragos Constantin at the 9th EARSeL SIG Imaging Spectroscopy workshop in Luxembourg at the session for Remotely Piloted Aircraft Systems (RPAS) based hyperspectral remote sensing of vegetation 16/Apr/2015.

Zusammenfassung: Luftgestützte Fernerkundungstechnologien stellen effektive Methoden zur Erforschung und Detektion von Pflanzeneigenschaften dar. In dieser Studie wurde ein Hexakopter mit einer Miniatur-Hyperspektralbildkamera ausgestattet, welche 16 Kanäle im sichtbaren Bereich messen kann. Die einzelnen Hyperspektralbilder (HSI) wurden zu geo-rektifizierten und registriert Karten verrechnet, aus welchen die Daten zur Berechnung der spektralen Indices (SI) extrahiert wurden. Die SI´s wurden mit Pflanzeneigenschaften wie Blattstickstoffkonzentration (N_{conc}), Chlorophyll- (CHL_{tot}) und totalem Pigmentgehalt ($Pigm_{tot}$), Bedeckungsgrad (CC) und Blattflächenindex (LAI) korreliert. Die Beziehung von N_{conc} und CHL_{tot} wird im Detail unter Berücksichtigung von Messungsschwierigkeiten, wie der Wechselbeziehung zu LAI, und der Anwendung in Präzisionslandwirtschaft oder Pflanzenzüchtung diskutiert.

Deskriptoren: Hyperspektralkamera, unbemannte Luftfahrzeuge (UAV), Phänotypisierung, Präzisionslandwirtschaft,

Abstract: *Aerial hyperspectral remote sensing technologies provide effective methods for the exploration and study of plant and crop properties. In this study a custom made hexacopter was equipped with a small scale hyperspectral imaging (HSI) camera capable of measuring 16 bands in the visible range of the light. From single HSI images geo-rectified and registered maps were calculated and a selection of spectral indices (SI's) calculated from the provided data. The SI´s were correlated to crop traits such as leaf nitrogen (N_{conc}), chlorophyll (CHL_{tot})and total pigment concentration ($Pigm_{tot}$), canopy cover (CC) and leaf area index (LAI), measured in the field. The relationships to N_{conc}*

and CHL_{tot} are discussed in detail with respect to measurement constraints, such as the interrelationships to LAI and application for precision farming or breeding experiments.

Keywords: *hyperspectral camera, unmanned aerial vehicles (UAV), phenotyping, precision agriculture*

1 Introduction

Aerial hyperspectral remote sensing technologies provide effective methods for the exploration and study of plant and crop traits. The recent progress in miniaturization of imaging and processing modules enables the use of low-cost unmanned aerial vehicles (UAV) as sensor carriers (COLOMINA & MOLINA 2014). They offer a great potential for local area remote sensing applications, such as for agriculture, forestry, mining industry and hydrological applications. For agriculture in particular they will allow non-destructive detection of plant biophysical and chemical properties (MULLA 2013, LIEBISCH *et al.* 2014, LIEBISCH *et al.* 2015) with a high spatial and temporal resolution relevant for precision farming and for agricultural research and phenotyping in particular (WALTER *et al.* 2015).

We present a case study conducted over the Field Phenotyping Platform (FIP) (presented by KIRCHGESSNER *et al.,* at this workshop) at the ETH Zürich research station for plant sciences in Eschikon, Lindau (KIRCHGESSNER *et al.* 2015), as collaboration between EPFL TOPO laboratory, Gamaya Company and the ETHZ Crop Science Laboratory. The aim of this case study was to test the determination of crop properties and phenotypes as related to spectral characteristics by using a novel hyperspectral imaging (HSI) snapshot camera with 16 bands in the visible range developed by Gamaya, Lausanne, Switzerland (2014).

2 Method

2.1 The sensor carrier

The UAV deployed during this study was a custom made hexa-copter with Pixhawk autopilot (PIXHAWK 2014) portrayed (**Figure 1**). The unit allows for execution of manual and automatic flights as well as a tight integration with the imaging system. The cameras were integrated together with an embedded computer assuring a proper triggering and synchronization of all the components. Moreover, the camera sensor head was accompanied by global navigation satellite system and inertial navigation system (GNSS/INS) constituting a compact all-in-one remote sensing system. The navigation and imaging systems were synchronized to provide precise position and orientation information for each acquired image that in turn speeds up the processing. In addition, the precise knowledge of exterior orientation parameters allows creating seamless orthomosaic-images and multispectral maps (**Figure 2**) without the need of establishing

ground control points which significantly reduces the time and resources needed for application in the field.

3 The sensor and spectral data analysis

Gamaya provides turnkey UAV-optimised hyperspectral imaging solutions for industrial applications and develops applications for precision agriculture and other purposes. In this study a model with 2MP sensor (2048 x 1088 px) spatial resolution and 16 bands in the visible range (450-650 nm) and a monochrome model with the same resolution were used. Each camera has a size of 4x4x6 cm and a weight of 100-120 g depending on mounted optic. In particular, the snapshot imaging model allows for the use of modern image processing based techniques for the geometric registration of HSI data. The hyperspectral data cubes were evaluated and plot data corresponding to the ground sampling points extracted with ENVI 5.1 (Exelis, Inc, US). Subsequently, spectral data from a set of 34 plots (4 m^2) including a range of different crops (soybean, sunflower, maize and buckwheat) were plant properties were determined. We calculated eight spectral indices (SI) reported for visible range (**Table 1**).

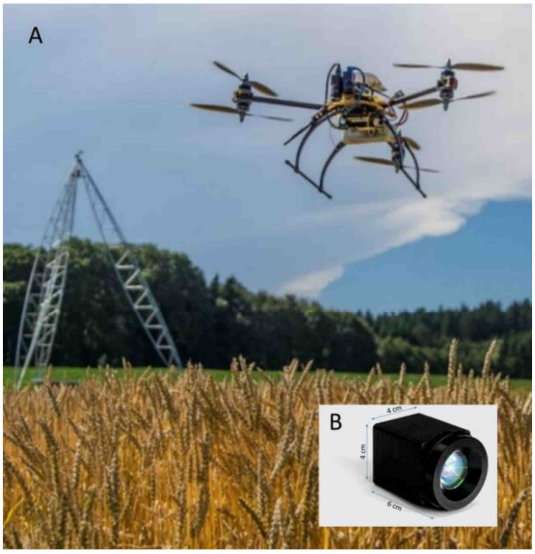

Figure 1: UAV Hexacopter mounted with two Gamaya cameras in the FIP field (A) and the camera in detail (B)

Table 1: A Selection of spectral indices in the visible range of the spectrum and related references.

Name	Abbreviation	Equation	References
Green leaf index	GLI	$(2\times R_g - R_r - R_b)/(2\times R_g + R_r + R_b)$	HUNT *et al.* (2011)#
Summed green reflectance	SGR	$\sum R_{500\text{-}599}$	(PU 2011)
Vegetation index green	VIgreen	$(R_g - R_r)/(R_g + R_r)$	THENKABAIL *et al.* (2012)
Carotenoid reflectance index 550	CRI1	$(1/R510) - (1/R_{550})$	GITELSON *et al.* (2002)
Photochemical reflectance index	PRI	$(R_{531} - R_{570})/(R_{531} + R_{570})$	GAMON *et al.* (1992)
Red-green ratio	RGR	R_r/R_g	SIMS & GAMON (2002)#
Plant pigment ratio	PPR	$(R_{550} - R_{450})/(R_{550} + R_{450})$	WANG *et al.* (2004)
Triangular greenness index	TGI	$-0.5[(W_{670} - W_{480})(R_{670} - R_{550}) - (W_{670} - W_{550})(R_{670} - R_{480})]$	HUNT *et al.* (2011)

R = reflectance, subscript numbers represent wavelength, b = blue (450-520 nm), g = green (520-600 nm), r = Red (630-690 nm), W = wavelength

calculated as narrow band here using the narrow bands closest to the band centre of the camera bands given above.

4 Field experiment

For the 34 plots (4 m^2) shown in **figure 2** including a range of different crops (soybean, sunflower, maize and buckwheat) a set of seven plant traits were determined. The investigated traits were leaf nitrogen, chlorophyll and total pigment concentration (in mg g^{-1}), canopy cover (fraction of plant per area of soil %), leaf area index (m^2 m^{-2}), SPAD (leaf greenness) and canopy height (cm). Further methodological details can be found in LIEBISCH *et al.* (2014 and 2015).

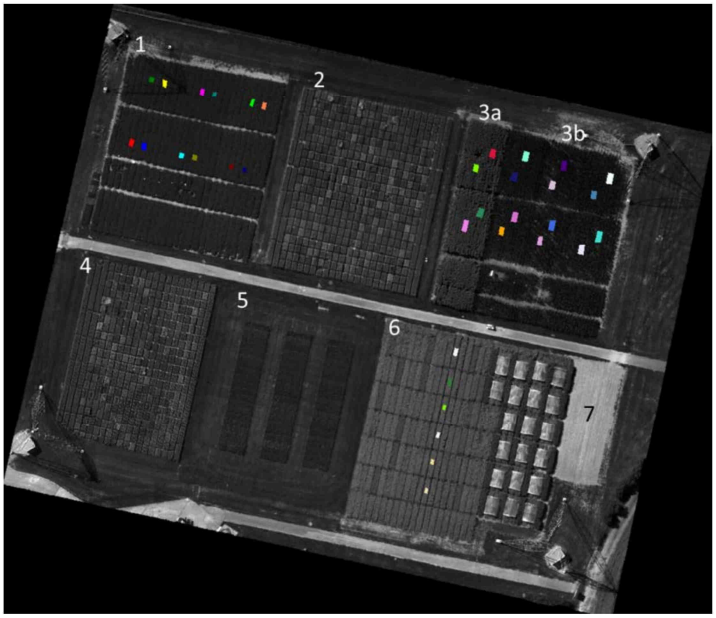

Figure 2: Test location at the FIP site at the ETH Zürich research station in Eschikon, Lindau. A total of 7 crop species was cultivated with a varying extend of genotypes, respectively: 1 soy bean, 2 +4 winter wheat, 3a sun flower, 3b maize, 5 red clover and 6 buckwheat. The location of the 34 sampling plots is indicated by small squares (ROIs) in the image. The intermediate soil cover is a mulch meadow and an open soil area was integrated (7).

5 Results and Discussion

The presented results reflect measurements at a single measurement date with recommended nutrient input during growth, assuming no restrictions in nutrient availability. Therefore, the observed variances within a given crop species were rather small and represent mostly genotype differences. The variability found between the investigated crop species were useful to deduce general relationships between plant traits and remote detected spectral indices and there application in agricultural settings. For the use as decision support crop specific relationships need to be established considering controlled input experiments.

Integrating several crops for each of the eight plant traits good to very good (marked by ***) relationships to the remote detected SIs (**Table 1**) were identified and are reported as coefficients of correlation in **table 2**. Three examples for a linear relationship between remote detected SI and ground observed plant traits are plotted in detail in **figure 3**. Interestingly, for the three strongly interlinked plant traits leaf nitrogen concentration (N_{conc}), leaf total chlorophyll concentration (CHL_{tot}) and leaf SPAD value (SPAD) different SIs were found to be superior for detection. PRI was found to be the best indicator for N_{conc}, while it was not related to CHL_{tot} and SPAD values. A map of the observed PRI and the respective N concentration is shown in Figure 5A and B. SGR was the best indicator for CHL_{tot} and $Pigm_{tot}$, whereas it was well correlated to SPAD too, but only weakly related to leaf N_{conc}. The best remote SI for SPAD was the TGI, which was well correlated to CHL_{tot} and $Pigm_{tot}$, but not to N_{conc}.

Canopy cover and LAI, two traits reflecting canopy architecture were best represented by PRI and TGI reflecting a well-known trade off compromising the leaf biochemical information included in the signal. However, the SGR was not correlated to CC and LAI and thus could potentially be used as independent indicator for CHL_{tot}. For N_{conc} detection a correction for the present CC or LAI by means of the independent TGI could improve reliability of remote detection of N_{conc}, irrespective of the present crop (r^2 = 0.54***, data not shown). The best use of HSI data for precision farming such as detection of trait variation in the field or trait detection for breeding should be subject of further studies.

Table 2: Correlation coefficients of spectral indices and plant traits measured in the field (Ground truth).

Spectral index	**Ground truth data**						
trait	N_{conc}	CHL_{tot}	$Pigm_{tot}$	CC	LAI	SPAD	Height
unit	mg g^{-1}	mg g^{-1}	mg g^{-1}	%	m^2 m^{-2}		cm
n	34	33	33	34	34	34	34
GLI	0.56 ***	0.59 ***	0.58 ***	0.43 *	0.35 *	0.17 ns	-0.15 ns
SGR	-0.34 *	-0.95 ***	-0.94 ***	0.13 ns	0.2 ns	-0.68 ***	-0.33 ns
VIgreen	0.64 ***	0.46 **	0.45 **	0.58 ***	0.51 **	-0.01 ns	-0.3 ns
CRI1	0.04 ns	0.78 ***	0.79 ***	-0.3 ns	-0.36 *	0.74 ***	0.39 *
PRI	0.71 ***	0.23 ns	0.21 ns	0.78 ***	0.71 ***	-0.3 ns	-0.5 **
RGR	-0.64 ***	-0.47 **	-0.46 **	-0.58 ***	-0.51 **	0 ns	0.28 ns
PPR	0.54 ***	0.61 ***	0.6 ***	0.4 *	0.31 ns	0.2 ns	-0.12 ns
TGI	0.07 ns	-0.83 ***	-0.83 ***	0.58 ***	0.62 ***	-0.89 ***	-0.58 ***

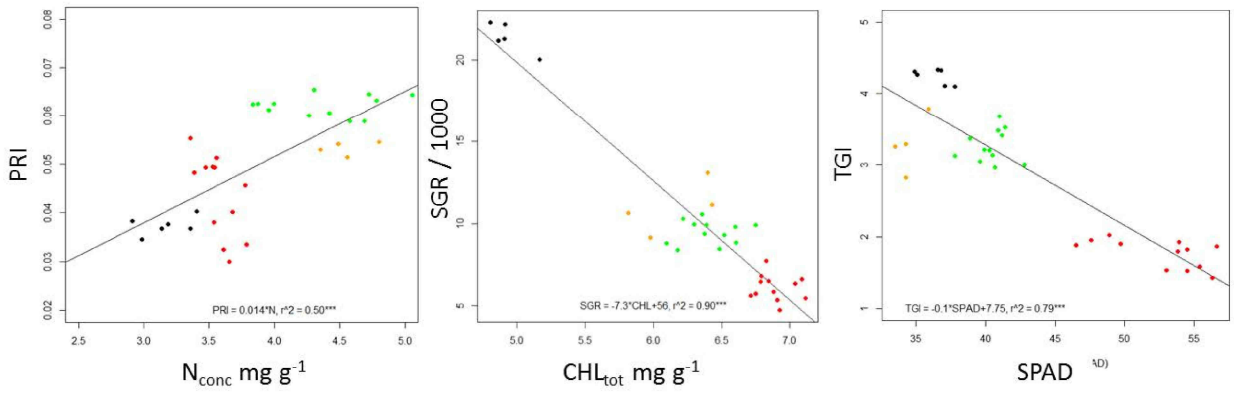

Figure 3: Linear relationship between the three SI´s PRI, SGR and TGI to N_{conc}, CHL_{tot} and SPAD, respectively. The colored circles represent maize (red), sun flower (orange), soy bean (green) and buckwheat (black).

The spatial resolution obtained with the investigated sensor at 30 m altitude seems to be sufficient to detect small plot experiments and to some extend single plants and thus is applicable for phenotyping experiments for plant breeding (**Figure 4**). At this scale of resolution it may partially be possible to disentangle soil and plant signals by means of segmentation as shown in Figure 4B (black = non plant pixels). However, the ground pixel size of 5-7 cm as observed in this study still results in mixed pixels, which may compromise the accuracy and precision of the remote indicators derived from the HSI data. Similar effects were discussed by LIEBISCH *et al.* (2015) for NIR, RGB and thermal imaging. Flying at lower altitudes may improve the spatial resolution if needed.

Although only in the visible range the spectral resolution of the investigated sensor was sufficient to calculate several narrow band SI´s found to reliably detect plant traits. The very high correlation to SPAD and CHL_{tot} indicates its superiority in contrast to broad band or consumer grade cameras (LIEBISCH *et al.* 2015, HUNT *et al.* 2011). Additionally, the availability of the 16 spectral bands allowed calculating at least partially independent SI´s which might enable a better remote field diagnosis in the future by using different trait indicators in combination (LIEBISCH *et al.* 2014). An even higher spectral range, particularly including the near infrared range is desirable as it will allow using a wider selection of SI´s. This will offer detection of other traits, such as water or phenol contents of plants or may eventually be superior for plant trait detection.

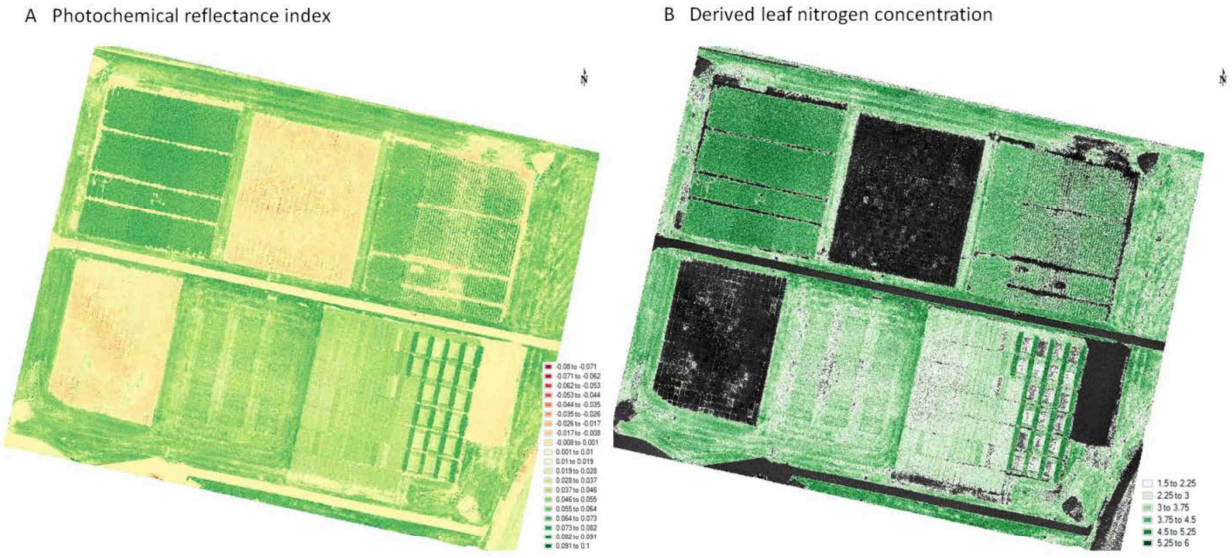

Figure 4: PRI map calculated from the HSI cube (left) and leaf nitrogen concentration (mg g^{-1}) map (right) as derived from its relationship to PRI (N_{conc} = PRI/0.014). Black pixels (N_{conc} < 1.5 mg g^{-1} corresponding to PRI < 0.021) represent non plant pixels.

6 Conclusion and outlook

The 16 band visible range camera was successfully tested in an agricultural setting. From the investigated spectral indices reliable indicators for all tested plant traits were identified. Particularly, the detection of leaf nitrogen and total chlorophyll concentration

was realized by means of the photochemical reflectance index and the sum of green reflectance respectively. However, for application in precision farming a species specific testing with variable nitrogen inputs would be important. A higher spectral range and advanced post processing are likely to improve the applicability of HSI in agriculture.

Acknowledgment

We thank A. Rieder and J. Heyer for the ground truth measurements and lab analyses during the measurement campaign in July 2014 supported by a grant of the Swiss University Conference and the ETH - Board in the frame of the Swiss Earth Observatory Network (SEON). We also thank H. Zellweger and N. Kirchgessner for their precious help for this project.

References

COLOMINA I., MOLINA P. (2014): Unmanned aerial systems for photogrammetry and remote sensing: A review. Journal of Photogrammetry and Remote Sensing 92, 79-97.

GAMAYA (2014): Accessed 12.12.2014, http://www.gamaya.com.

GAMON J.A., PEÑUELAS J., FIELD C.B. (1992): A narrow-waveband spectral index that tracks diurnal changes in photosynthetic efficiency. Remote Sensing of Environment 41, 35-44.

GITELSON A.A., ZUR Y., CHIVKUNOVA O.B., MERZLYAK M.N. (2002): Assessing Carotenoid Content in Plant Leaves with Reflectance Spectroscopy¶. Photochemistry and Photobiology 75, 272-281.

HUNT E.R., DAUGHTRY C.S.T., EITEL J.U.H., LONG D.S. (2011): Remote sensing leaf chlorophyll content using a visible band index. Agronomy Journal 103, 1090-1099.

KIRCHGESSNER N., LIEBISCH F., HUND A., WALTER A. (2015): Field imaging platform (FIP) – an automated system for plant phenotyping in the field. 21. Workshop Computer-Bildanalyse in der Landwirtschaft und 3. Workshop Unbemannte autonom fliegende Systeme (UAS) in der Landwirtschaft am 7. Mai 2015 Braunschweig.

LIEBISCH F., KIRCHGESSNER N., SCHNEIDER D., WALTER A., HUND A. (2015): Remote, aerial phenotyping of maize traits with a mobile multi-sensor approach. Plant Methods 11, 9.

LIEBISCH F., KÜNG G., DAMM A., WALTER A. (2014): Characterization of crop vitality and resource use efficiency by means of combining imaging spectroscopy based plant traits. Workshop on Hyperspectral Image and Signal Processing: Evolution in Remote Sensing. IEEE International, 24-27 June, Lausanne, Switzerland.

MULLA D.J. (2013): Twenty five years of remote sensing in precision agriculture: Key advances and remaining knowledge gaps. Biosystems Engineering 114, 358-371.

PIXHAWK (2014): Accessed 12.12.2014, https://pixhawk.ethz.ch/.

PU R. (2011): Detecting and mapping invasive species by using hyperspectral data. In: Thenkabail, P.S. (Ed.), Hyperspectral remote sensing of vegetation. CRC Press, Boca Raton.

SIMS D., GAMON J. (2002): Relationships between leaf pigment content and spectral reflectance across a wide range of species, leaf structures and developmental stages. Remote Sens Environ. 81, 337 - 354.

THENKABAIL P.S., LYON J.G., HUETE A. (2012): Hyperspectral remote sensing of vegetation. CRC Press, Taylor and Francis Group, Boca raton.

WALTER A., LIEBISCH F., HUND A. (2015): Plant phenotyping: from bean weighing to image analysis. Plant Methods 11, 14.

WANG Z.J., WANG J.H., LIU L.Y., HUANG W.J., ZHAO C.J., WANG C.Z. (2004): Prediction of grain protein content in winter wheat (Triticum aestivum L.) using plant pigment ratio (PPR). Field Crops Research 90, 311-321.